
ANALYSIS OF DARK MATTER HALO STRUCTURE FORMATION IN N -BODY SIMULATIONS WITH MACHINE LEARNING

Jazhiel Chacón

Centro de Investigación en Computación, Instituto Politécnico Nacional,
07738, Ciudad de México, México
Instituto de Ciencias Físicas, Universidad Nacional Autónoma de México,
62210, Cuernavaca, Morelos, México.
chacon12021@cic.ipn.mx

Isidro Gómez-Vargas

Instituto de Ciencias Físicas, Universidad Nacional Autónoma de México,
62210, Cuernavaca, Morelos, México.
igomez@icf.unam.mx

Ricardo Menchaca Méndez

Centro de Investigación en Computación, Instituto Politécnico Nacional,
07738, Ciudad de México, México.
ric@cic.ipn.mx

J. Alberto Vázquez

Instituto de Ciencias Físicas, Universidad Nacional Autónoma de México,
62210, Cuernavaca, Morelos, México.
javazquez@icf.unam.mx

March 17, 2023

ABSTRACT

The properties of the matter density field in the initial conditions have a decisive impact on the features of the large-scale structure of the Universe as observed today. These need to be studied via N -body simulations, which are imperative to analyze high density collapsed regions into dark matter halos. In this paper, we train Machine Learning algorithms with information from N -body simulations to infer two properties: dark matter particle halo classification that leads to halo formation prediction with the characteristics of the matter density field traced back to the initial conditions, and dark matter halo formation by calculating the Halo Mass Function (HMF), which offers the number density of dark matter halos with a given threshold. We map the initial conditions of the matter density field into classification labels of dark matter halo structures. The Halo Mass Function of the simulations is calculated and reconstructed with theoretical methods as well as our trained algorithms. We test several Machine Learning techniques where we could find that the Random Forest and Neural Networks proved to be the better performing tools to classify dark matter particles in cosmological simulations. We also show that it is not compulsory to use a high amount of data to train the algorithms in order to reconstruct the HMF, giving us a very good fitting function for both simulation and theoretical results.

Keywords Numerical Simulations, N -body systems, Machine Learning, Neural Networks, Cosmology · Machine Learning

1 Introduction

By studying the cosmological structure formation in the standard model, also known as Λ CDM, we are able to determine that the total amount of the Universe is divided among several constituents: visible matter (baryonic matter), which takes about 4.9 % of the total amount; neutrinos and photons which today are estimated that from less than 0.1% of the total content; dark matter, a hypothetical constituent of the Universe with purely gravitational interaction which collapses into filaments, halos and structures that eventually ended up merging the visible matter that creates galaxies and adds up about 23% of the total content of the Universe and finally dark energy, another hypothetical constituent, but this one being the responsible for the current accelerated expansion of the Universe, with the remaining 72 % of the total content of the Universe [3].

The presence of dark matter and dark energy, the so called ‘dark sector’ of the Universe, can be inferred from observational evidence of large-scale structures, which can be studied with analytical and semi-analytical models. Nevertheless, only numerical simulations are capable to emulate the small scale structures and sub-structures observed in the Universe, that give rise to a cosmic network of filaments, voids and groups. These structures act as gravitational wells around the visible matter, which eventually merge visible matter to create clusters of galaxies, quasars and gas clouds.

Using numerical simulations as virtual environments, we can evaluate and evolve a set of initial conditions of matter and energy that will eventually end up merging the structures as observed today by different telescopes and available probes. These environments can be considered as virtual laboratories that allow us to study different candidates of dark matter and dark energy. However, until a few years ago, numerical simulations were very restrictive in terms of computational resources, and only accessible to a few research groups. In this regard, there has been a rising amount of alternative methods, hardware and algorithms that would allow to lower the computational resources required to carry a full run of a cosmological simulation. Using artificial intelligence and other machine learning methods is becoming more accepted to model relevant features in numerical simulations. Within this area of study, there has been a variety of tasks and hardware development to enhance the analysis of cosmological structure formation and data. Some of these methods range from classification, clustering, regression, statistics and optimization among others [11, 12, 35, 15, 23, 18, 5, 19, 28].

The main idea presented in this work was described in [7] and originally based on the studies first made in [20], however, this new approach was carried out on larger N -body simulations which increase the dataset with more dark matter particles and we tested them on a variety of machine learning algorithms. Hence we obtained improved results compared to those achieved in the previous work, also because the important statistics, such as the Matter Power Spectrum, which remain intact even with the change in scale. Implementing a wide variety of machine learning algorithms, that can be used for classification, helps to test their efficiency and viability in terms of computational cost, therefore we evaluated their classification performance and their computational runtime. We find out how much information the features in the initial conditions provide in order to determine the formation of dark matter halos in cosmological simulations. In addition, to explore another application in this cosmological field, we implement a neural network to reconstruct the Halo Mass Function given only a few of points from simulations, which in most cases are computationally expensive to produce.

The content of this paper is as follows. In Section 2, we describe briefly the ML classification methods. In the sections 3 and 4 we describe how we used our dataset as a binary classification problem. For this purpose, we present a dark matter particle halo formation framework, which uses information about local density field features in the initial conditions of the simulation, and the final dark matter halo formation. Finally, in Section 5 we present our discussion of the results achieved.

2 Machine Learning algorithms

Machine Learning (ML) is the field of Artificial Intelligence that is focused on the statistical modeling of data. Common tasks in ML are classification, clustering, pattern recognition and time series analysis, among others. In this paper, we use ML algorithms to perform the classification of particles from N -body simulations in order to know whether they are within a dark matter halo, or they are not. Then, we briefly introduce the algorithms used in this work.

2.1 Logistic regression

Logistic regression, or logit regression, is a linear model for classification. It is one of the pioneer classification algorithms in Machine Learning, which relies its mechanism on assigning, to each instance, a probability of belonging to a particular class using the logistic function (also called sigmoid):

$$\sigma(x) = \frac{1}{1 + e^{-x}}. \quad (1)$$

This algorithm works in the same way as a linear regression, with the difference of converting its outputs into probabilities using the logistic function. We can describe the logistic regression as follows:

$$\hat{p} = \sigma(\theta^T \cdot x), \quad (2)$$

where θ represents the straight-line parameters and x the features of the input data. Therefore, the classification y_{pred} is given by:

$$y_{\text{pred}} = \begin{cases} 0 & \text{if } \hat{p} < 0.5 \\ 1 & \text{if } \hat{p} \geq 0.5 \end{cases}, \quad (3)$$

where 0 and 1 are two different classes.

2.2 Bayes classifier

A Bayes classifier obtains the conditional probability of each class C_i given a set of n attributes $A = A_1, \dots, A_n$ through the Bayes rule:

$$P(C_i|A) = \frac{P(C_i)P(A|C_i)}{P(A)}, \quad (4)$$

where the associated parameters are the prior probability for each class $P(C_i)$ and the conditional probability for each attribute given a class $P(A|C_i)$; these parameters can be estimated from the dataset using frequencies, i. e., this is a frequentist approach of the Bayesian rule.

The simplest Bayes classifier, known as Naive-Bayes, assumes that the attributes are conditionally independent; however, in several datasets, this condition is not satisfied and for this reason, some proposals have emerged that are its extensions, such as the Naive-Bayes complement [31], Gaussian Naive-Bayes [8] and multimodal Naive-Bayes [21]. In this work, we use these mentioned extensions and the classical Naive-Bayes algorithm.

2.3 Support Vector Machines

A Support Vector Machine (SVM) is a supervised learning method that uses separating hyperplanes in high-dimensional spaces to perform classification. It is particularly useful for solving problems where the number of features exceeds the number of observations, and the data points are not easily separable.

The primary concept behind SVM is to identify the hyperplane that separates the data points of distinct classes to the maximum extent possible. This hyperplane is chosen in a way that maximizes the margin, which refers to the distance between the hyperplane and the nearest data points of each class. The support vectors are the data points that are closest to the hyperplane and are used to define the hyperplane. The objective of SVM is to determine the optimal boundary between the potential classes. While there are several hyperplanes that could potentially separate the classes, the best option is the one that has the greatest distance between the points of different classes, known as the maximum-margin hyperplane. Therefore, SVM involves a maximization problem.

SVMs have the ability to handle high-dimensional data and they are robustness to overfitting. A concise explanation about SVM is available in Ref. [26] and for mathematical details we recommend the Ref. [33].

2.4 Decision trees and random forest

Decision trees refer to a paradigm of learning based on approximating discrete target functions, in which the learned function is represented by a decision tree [22]. The elements of a decision tree are the roots (where the data is stored), the branches (the path the tree takes to make decisions) and the nodes (consisting of sets of elements that have a determined characteristic after a decision is made). Given a dataset, we can calculate the inconsistency within the set, or in other words, find its entropy in order to divide or split the set until all data are within a given class [30]. When

there exist a large number of decision trees that operate together as an ensemble, we are referring to the Random Forest algorithm [16]. The randomness of this algorithm comes from the fact that operations and predictions from the forest are not hierarchically taken, but a subset of elements (like the number of trees, number of attributes, length of data, etc.) is taken in a random way.

2.5 Artificial Neural Networks

Artificial neural networks (ANNs) are able to model large and complex datasets and any nonlinear function [17]. They are computational models that represent the synapse of biological neurons through interconnected layers of units called neurons or nodes, which make up its basic information processing elements. In the simplest type of neural network, the Multi-layer perceptron (MLP) (also called feedforward neural network), there are three types of layers: an input layer that receives the input, hidden layers responsible for extracting patterns and producing nonlinearity effects, and finally the output layer that presents the results of the prediction.

For a full background of neural networks we recommend the references [14, 4, 25]; or, for a basic introduction in the cosmological context, see [32].

3 Dark matter halo formation as a binary classification framework

Using the set of numerical simulations described in [6], we are able to obtain a relational database that includes information about the merged dark matter halos at cosmological time $z = 0$. We obtained numerical features within the initial conditions of the dark matter particles used for the simulations. Additionally, we identified host halos and sub-halos that allow us to associate dark matter substructures to larger merged halos, in order to determine a dark matter halo mass classification threshold.

3.1 Data selection

We performed a simulation with the cosmological code GADGET-2, [34] assuming a Λ CDM Universe. The data output was designed such that the dimensionless density parameters were $\Omega_m = 0.268$, $\Omega_\Lambda = 0.683$, $\Omega_b = 0.049$, $h = 0.7$ and with a gravitational softening of $\epsilon = 0.89$ kpc. The total number of dark matter particles is 192^3 , each with a mass of $1.3 \times 10^9 M_\odot$ in a box of comoving length $L = 50h^{-1}$ Mpc running from $z = 23$ to $z = 0$. To identify dark matter halos and subhalos we use ROCKSTAR halo finder [2]. The final snapshot has a total of 4000 dark matter halos whose masses fall within the range ($10^{11} \leq M/M_\odot \leq 10^{14}$). This given mass will be used as the binary threshold to classify dark matter particles: if a selected particle falls within a halo with mass between $10^{11} \leq M/M_\odot \leq 10^{14}$, then the dark matter particle will have a classification label of 1, otherwise if this condition is not met, the dark matter particle will have a classification label of 0.

The properties from the density field of the initial conditions of the simulation serve as an input data to our ML models. The attributes of the dataset are calculated from analytical works related to the halo mass function (HMF) by Press-Schechter [29]. This function predicts the number density of dark matter halos depending on their mass and the density field. The density generates a halo of a certain mass M at a given redshift z . If it exceeds a critical value $\delta_c(z)$, these values will be called overdensities at redshift z .

The core idea is that the dark matter halos enclose their mass in a dense spherical region, where the density contrast will be given by the following relation:

$$\delta(\mathbf{x}) = \frac{\rho(\mathbf{x}) - \bar{\rho}}{\bar{\rho}}, \quad (5)$$

where $\bar{\rho}$ is the average matter density of the Universe. For a sphere of radius R , the overdensity is defined as follows [9]:

$$\delta(\mathbf{x}, R) \equiv \int d^3\mathbf{x}' \delta(\mathbf{x}') W_R(\mathbf{x} - \mathbf{x}'). \quad (6)$$

In eq. (6), W_R is a window function of the *top hat* model, given by:

$$W_R = \begin{cases} \frac{3}{4\pi R^3} & \text{if } |\mathbf{x}| \leq R \\ 0 & \text{if } |\mathbf{x}| > R. \end{cases} \quad (7)$$

A window function with radius R and volume V corresponds to a mass scale $M = \bar{\rho}V(R)$. The expected value of the overdensity in eq. (6) is the normalization term of the power spectrum σ_R , which is defined by the following relation:

$$\sigma_R^2 = \langle \delta^2(\mathbf{x}, R) \rangle. \quad (8)$$

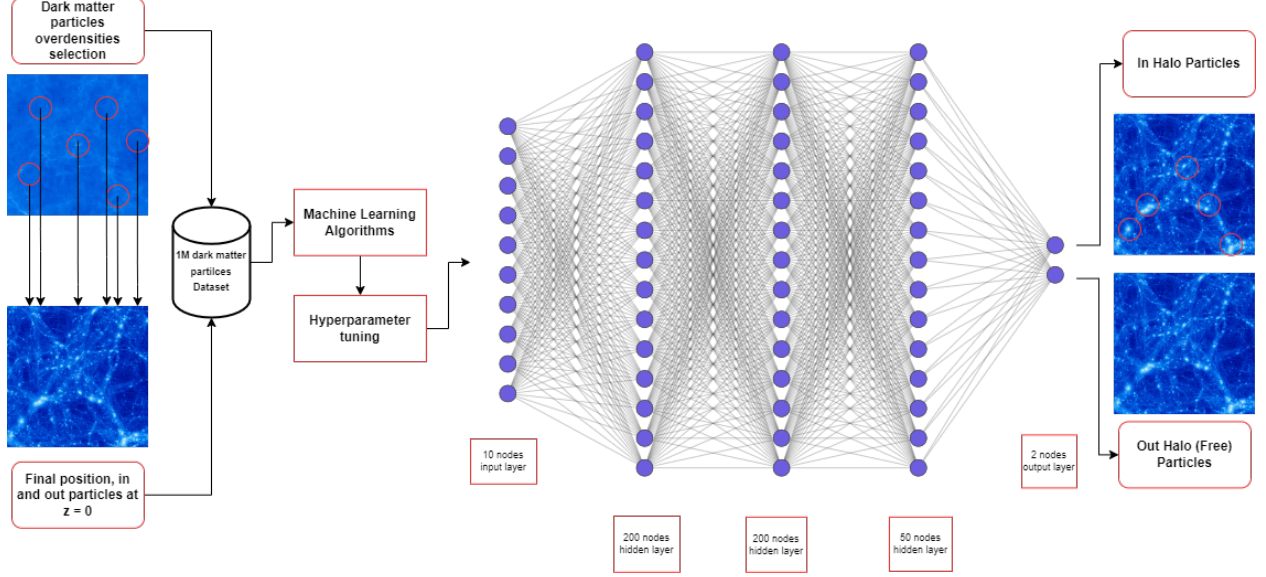


Figure 1: Diagram of the method to select the properties of the initial density field conditions that will eventually form the structure in the simulation. The process starts by extracting properties of the initial conditions in the local neighborhood of the density field around dark matter particles and associate them with the final position in the halo distribution. The final classification `Not in halo`, `In Halo` depends on the mass threshold chosen to determine whether a dark matter particle will belong to a halo or if it is not bound to any other object.

The attributes that we are able to define with eqs. (6) and (7) allow us to create a structured database, with the information of overdensities at different radius R values, derived from a mass scale M_R centered on the position of a particle, from the initial conditions at redshift $z = 23$. This allows us to create a ten-component vector, namely, $\delta_1, \dots, \delta_{10}$, with their respective classification label. The mass range was selected taking into account two main features: first, the data we selected take into account the average of mass range for the halos found; second, the mass range was also a calculation from the approximation of the spherical collapse model, which gave us the range of $(10^{11} \leq M/M_\odot \leq 10^{14})$ for the threshold.

4 Methodology

The framework described in the previous section allowed us to implement the ML algorithms described in Section 2, all of them available in the Python libraries: `Scikit-Learn` [27] and `TensorFlow` [1]. The dataset consists of one million (1,000,000) randomly selected dark matter particles, each of them with a ten-component vector, whose features are the overdensities $\delta_1, \dots, \delta_{10}$ at different values of radius R . This selection upscales the previous work [7], where we used 50,000 randomly selected particles, up to 2 orders of magnitude, allowing our models to be more competitive with the training and validation tests. Since the particles are randomly sampled from the simulation, it is unlikely they are in some way correlated, this allows us to reduce the bias and overfitting at the moment of evaluation in the test sets. Figure 1 shows a schematic picture for our entire pipeline to train our algorithms.

All classification algorithms were fine-tuned by performing a hyperparameter grid search. This grid has a variety of hyperparameters depending on the algorithm we were testing. Each algorithm will have as an outcome the accuracy, precision, recall and F_1 -score as their performance metrics. The algorithms were successfully trained and we tested their ability to predict the final label of the particles in the test set, which is compared with the real labels in order to obtain the performance of each algorithm. This evaluation was carried out under the Receiving Operation Characteristics (ROC) curve [10] along with the Area Under Curve (AUC).

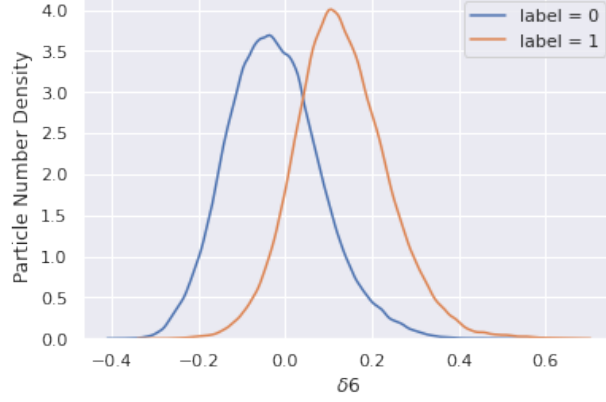


Figure 2: Dark matter particle number density distribution according to a defined overdensity δ_5 . It can be noticed that our dataset is evenly distributed, we have more particles in the `In Halo` class rather than the `Not In Halo` class. Given this, we can use both ROC and PR curves to test the accuracy of the algorithms.

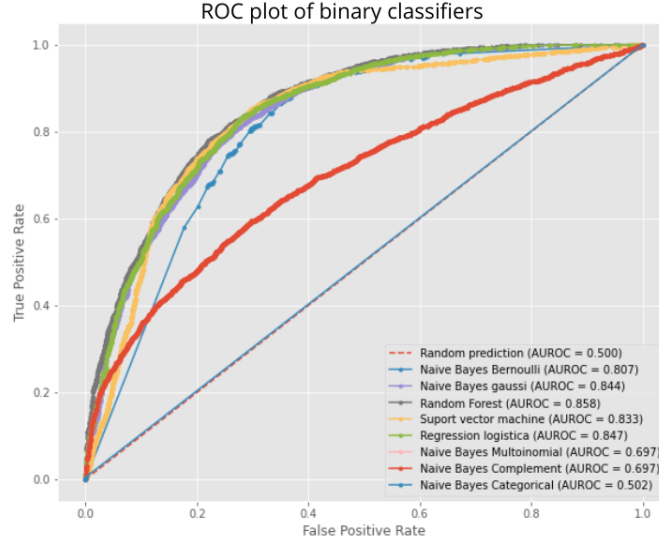


Figure 3: ROC and PR curves of 8 out of the 9 ML classifiers used. It can be seen that the performance rate drops drastically, especially for the Naive Bayes-like classifiers. This is related to the case that some of these classifiers perform better with categorical data rather than numerical data. These classifiers may not be used as predictors.

5 Results

5.1 Dark matter particles classification

We were able to test nine binary classification algorithms using the N -body simulation data as input. In figure 2 we plot the dark matter particle distribution labels, where we observe how our selection is evenly distributed. This is an indicator to verify the results using the ROC curve and the AUC score, resulting in the performance plotted in figure 3. Additionally, we detail the performance metrics in Table 1. It is interesting to point out that the best performing classifier was the Multi-Layer Perceptron, which obtained a high accuracy of 80%, and that its closest contender was the random forest, with 78% accuracy.

On the other hand, logistic regression has good performance in terms of accuracy and execution time, this is due to the own algorithm's design, which is performing quick calculations with the sigmoid function, but it lacks precision, which means it is predicting a high amount of false positives. Support vector machines are another example where having a high accuracy does not imply having high precision, this low percentage is giving rise to almost 50% data as false positives. These results are not optimal for prediction purposes.

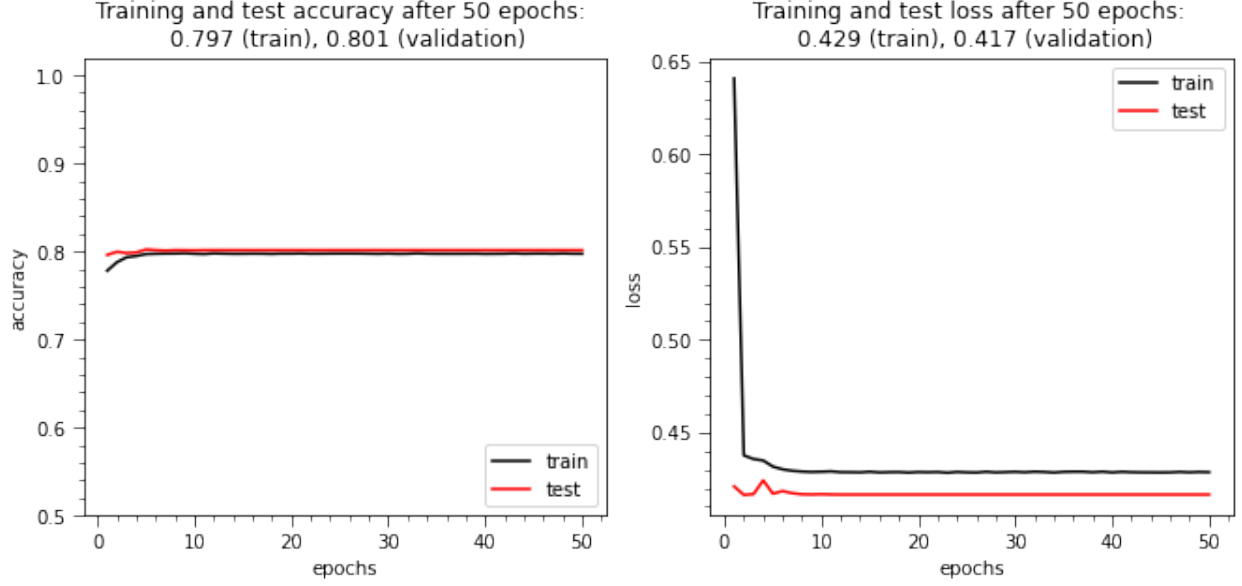


Figure 4: *Left.* Accuracy plot for the training and test sets for the Multi-Layer Perceptron through 50 epochs. The low gap between training and test sets is an indicator of how well is performing our neural network. *Right.* Loss function behavior on the training and test sets of the Multi-Layer Perceptron.

Table 1: Metrics and scores of binary classifiers

Classifier	Accuracy	Precision	Recall	F ₁ score
Logistic Regression	0.722	0.498	0.711	0.727
Naive Bayes Gaussian	0.718	0.516	0.757	0.748
Naive Bayes Bernoulli	0.699	0.495	0.757	0.730
Naive Bayes Multinomial	0.611	0.316	0.554	0.527
Naive Bayes Complement	0.608	0.316	0.554	0.527
Naive Bayes Categorical	0.699	0.370	0.578	0.568
Support Vector Machines	0.723	0.473	0.753	0.702
Random Forest	0.785	0.767	0.792	0.792
Multi Layer Perceptron	0.806	0.764	0.794	0.794

Regarding other classifiers, even though they have a good performance overall, they fail to perform better on unseen data due to the low precision and recall, as it turns out, some of these classifiers are very well adapted to categorical data, like Naive Bayes Categorical or Multinomial, and since we used only numerical data, their precision is lower, this is an indicator to discard these types of algorithms as predictors in the test set.

An interesting result we obtained was with the neural network performance, in which we see the highest accuracy among all other algorithms tested. For this particular method, we use three hidden layers with 200, 200 and 50 nodes respectively, 50 epochs, 1024 as batch size, 0.2 for dropout value, sigmoid as activation function and with the Adam gradient descent algorithm. With this configuration, figure 4 shows a good performance for the neural network in the accuracy metric and in the loss function for the training and test sets. Furthermore, the Multi-Layer Perceptron obtained the highest metric values among all other classifiers, with a fairly low execution time. As we can observe from Figure 4, the training and test accuracy curves after 50 epochs are practically the same, which means that the neural network is correctly classifying unseen data and, additionally, the training and test loss values are diminishing after less than 10 epochs. This result is an indicator that our model is not overfitting.

5.2 Halo Mass Function reconstruction

We were also able to reproduce some interesting results regarding the Halo Mass Function (HMF) at redshift $z = 0$ with the ML algorithms. As we know, the halo number density in function of its mass is one of the main results that we

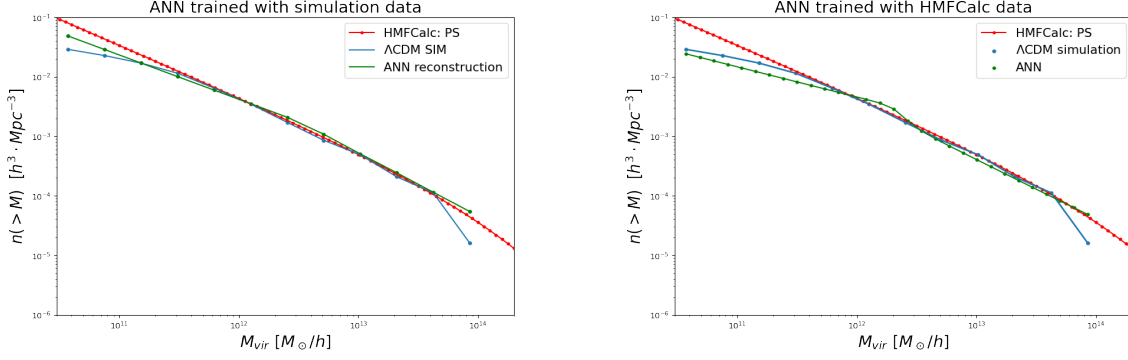


Figure 5: *Left*: Halo Mass Function reconstructed by the ANN (green line) trained and fitted with the Λ CDM simulation data (blue line). Since the ANN does not learn very well from the extreme values [13], it is visible that the ANN does not follow the pattern on values higher than $10^{13} M_{\odot}$ and fewer than $10^{11} M_{\odot}$. *Right*: Halo Mass Function reconstructed by the ANN (green line) trained and fitted with HMFCalc data (red line). We were able to upsample the initial datapoints available with this treatment.

want to focus when we evaluate a simulation output. The density profile has been widely studied since 1974, and one of the most important density profiles is the Press-Schechter profile [29], which was used in this work as a benchmark.

Since halo formation is hierarchical, the less massive halos merge to create the most massive halos. The HMF is often displayed in \log_{10} scale. This profile can be solved analytically using some parametric modifications of the top hat spherical collapse model. With this information, we use the parametric results of the Press-Schechter density profile with HMFCalc [24], an online tool to obtain the HMF with the Press-Schechter formalism, with initial conditions similar to the Λ CDM scenario of our simulation, as described in section 3.1.

Using only 13 data points from cosmological simulations, we were able to reconstruct the HMF with the ANN. Figure 5 shows the result of using only the ANN, where we can see how the reconstruction fits the data of the simulation as well as the theoretical curve of HMFCalc. On the left side we observe the HMF reconstructed with the training and fitting data from the Λ CDM simulation, whereas, on the right we upsampled the data available using the HMFCalc values from the Press-Schechter formalism. In figure 6 it is the result using both simulation and HMFCalc data as training and fitting data. Notice how the low sample points retrieved from the Λ CDM simulation are upsampled with the use of the MLP, because this algorithm is extrapolating data in order to achieve better results, fitting the HMF. Since we are using a 50Mpc boxsize, halo formation in the higher mass scale is somehow affected by this resolution. By using these two methods, we can predict higher mass halo merging, while in the lower bound, less massive halos are still within the range of the simulation, this may be due to the neural network does not learn very well from extreme values [13]. Nevertheless, the prediction of both algorithms fits in the $[10^{12} M_{\odot}, 10^{13} M_{\odot}]$ halo mass range. This result may seem contradictory, because it is known that in order to have a reliable result in the performance of an algorithm it is required to have a big amount of data, however the performance of both algorithms showed to be good in the higher bound mass values. The Multi-Layer Perceptron was trained in the middle range values and its prediction fits the results of both theoretical and simulated data.

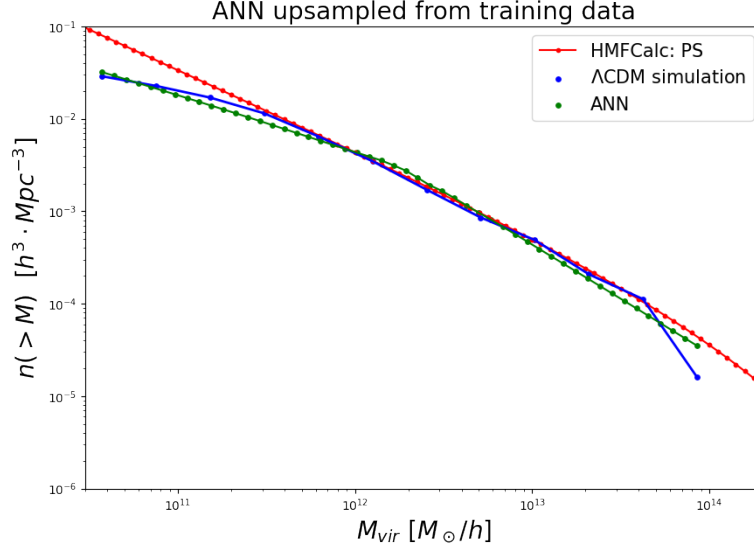


Figure 6: Halo mass function reconstruction with the ANN (green line), compared with both simulation data (blue line) and HMFCalc with a Press-Schechter profile (red line). As observed, we obtained few data from the simulation, however, with our implementation, it is possible to obtain more information with the Neural Network. The NN performs specially well in the $[10^{12}, 10^{13} M_{\odot}]$ range, whereas in the more extreme values, it tends to extrapolate the result with the simulated data.

6 Final discussion and future work

We were able to improve the results found in Reference [7] by implementing more classification algorithms to an enlarged data selected from a N -body cosmological simulation, our emphasis was to show a selected number of ML classifiers and see how well the performance showed on unseen data. As it turned out, some machine learning methods outperformed, like random forest and neural networks, since they rely more on iterative processes over numerical data to train and test their predictions, whereas categorical algorithms do not fit our binary classification purposes. We can conclude that our dataset, consisting of feature selection of the initial conditions of the dark matter density field together with the final halo formation, has enough information to provide an insight about the algorithms used as well as the physical properties within the data selected. The training process was refined up until it gets the best hyperparameters, and since the number of selected particles represents a bigger percentage of the total number of particles within the simulation, we observed an improvement in performance compared to our previous results.

Another important result is the HMF reconstruction using an ANN, with this framework, we can offer an alternative regarding the halo number density formation in cosmological simulations using a fairly low quantity dataset. There is no need to use a high amount of data for training, as the results fit especially well in the $[10^{12} M_{\odot}, 10^{13} M_{\odot}]$ halo mass range. This is specially true for the ANN architecture. We are encouraged to continue this work with deep learning techniques using image information and classification for N -body simulations in the near future.

Acknowledgments

J.Ch. would like to thank CONACYT for providing scholarship support and Brian Daniel Manzano Quechol for his help in the process of this work. IGV thanks the CONACYT postdoctoral fellowship and the support of the ICF-UNAM. J.A.V. acknowledges support from FOSEC SEP-CONACYT Ciencia Básica A1-S-21925, FORDECYT-PRONACES-CONACYT 304001 and UNAM-DGAPA-PAPIIT IN117723.

References

- [1] M. Abadi, A. Agarwal, P. Barham, E. Brevdo, Z. Chen, and et al. TensorFlow: Large-scale machine learning on heterogeneous systems, 2015. Software available from tensorflow.org.

- [2] P. S. Behroozi, R. H. Wechsler, and H.-Y. Wu. The ROCKSTAR Phase-space Temporal Halo Finder and the Velocity Offsets of Cluster Cores. *Astrophysical Journal*, 762:109, Jan. 2013.
- [3] C. L. Bennett, D. Larson, J. L. Weiland, N. Jarosik, G. Hinshaw, N. Odegard, K. M. Smith, R. S. Hill, B. Gold, M. Halpern, E. Komatsu, M. R. Nolta, L. Page, D. N. Spergel, E. Wollack, J. Dunkley, A. Kogut, M. Limon, S. S. Meyer, G. S. Tucker, and E. L. Wright. Nine-year Wilkinson Microwave Anisotropy Probe (WMAP) Observations: Final Maps and Results. *Astrophysical Journal, Supplement*, 208(2):20, Oct. 2013.
- [4] C. M. Bishop and N. M. Nasrabadi. *Pattern recognition and machine learning*, volume 4. Springer, 2006.
- [5] B. Buncher and M. Carrasco Kind. Probabilistic cosmic web classification using fast-generated training data. *Monthly Notices of the Royal Astronomical Society*, 497(4):5041–5060, Jul 2020.
- [6] J. Chacón, J. Vazquez, and R. Gabbasov. Dark matter with n-body numerical simulations. *Revista Mexicana de Física E*, 17:241, 07 [arXiv: 2006.10203].
- [7] J. Chacón, J. Vázquez, and E. Almaraz. Classification algorithms applied to structure formation simulations. *Astronomy and Computing*, 38:100527, 2022 [arXiv: 2106.06587v2].
- [8] T. F. Chan, G. H. Golub, and R. J. LeVeque. Updating formulae and a pairwise algorithm for computing sample variances. In *COMPSTAT 1982 5th Symposium held at Toulouse 1982*, pages 30–41. Springer, 1982.
- [9] S. Dodelson and A. P. L. . 1941-1969). *Modern Cosmology*. Elsevier Science, 2003.
- [10] T. Fawcett. Introduction to roc analysis. *Pattern Recognition Letters*, 27:861–874, 06 2006.
- [11] I. Gómez-Vargas, J. B. Andrade, and J. A. Vázquez. Neural networks optimized by genetic algorithms in cosmology. *Physical Review D*, 107(4):043509, 2023 [arXiv:2209.02685].
- [12] I. Gómez-Vargas, J. A. Vázquez, R. M. Esquivel, and R. García-Salcedo. Cosmological reconstructions with artificial neural networks. *arXiv preprint arXiv:2104.00595*, 2022.
- [13] I. Gómez-Vargas, J. A. Vázquez, R. Medel Esquivel, and R. García-Salcedo. Cosmological Reconstructions with Artificial Neural Networks. *arXiv e-prints*, page arXiv:2104.00595, Apr. 2021.
- [14] I. Goodfellow, Y. Bengio, A. Courville, and Y. Bengio. *Deep learning*, volume 1. MIT press Cambridge, 2016.
- [15] A. Hajian, M. A. Alvarez, and J. R. Bond. Machine learning etudes in astrophysics: selection functions for mock cluster catalogs. *jcap*, 2015(1):038, Jan. 2015.
- [16] T. Hastie, R. Tibshirani, and J. Friedman. *The elements of statistical learning: data mining, inference and prediction*. Springer, 2 edition, 2009.
- [17] K. Hornik, M. Stinchcombe, and H. White. Universal approximation of an unknown mapping and its derivatives using multilayer feedforward networks. *Neural networks*, 3(5):551–560, 1990.
- [18] H. M. Kamdar, M. J. Turk, and R. J. Brunner. Machine learning and cosmological simulations – ii. hydrodynamical simulations. *Monthly Notices of the Royal Astronomical Society*, 457(2):1162–1179, Feb 2016.
- [19] V. V. Kindratenko and R. J. Brunner. Accelerating cosmological data analysis with fpgas. In *2009 17th IEEE Symposium on Field Programmable Custom Computing Machines*, pages 11–18, 2009.
- [20] L. Lucie-Smith, H. V. Peiris, A. Pontzen, and M. Lochner. Machine learning cosmological structure formation. *Monthly Notices of the Royal Astronomical Society*, 479(3):3405–3414, 06 2018.
- [21] C. D. Manning. *Introduction to information retrieval*. Syngress Publishing, 2008.
- [22] T. M. Mitchell and T. M. Mitchell. *Machine learning*, volume 1. McGraw-hill New York, 1997.
- [23] B. P. Moster, T. Naab, M. Lindström, and J. A. O’Leary. GalaxyNet: Connecting galaxies and dark matter haloes with deep neural networks and reinforcement learning in large volumes. *arXiv e-prints*, page arXiv:2005.12276, May 2020.
- [24] S. G. Murray, C. Power, and A. S. G. Robotham. HMFcalc: An online tool for calculating dark matter halo mass functions. *Astronomy and Computing*, 3:23, Nov. 2013.
- [25] M. A. Nielsen. *Neural networks and deep learning*, volume 25. Determination press San Francisco, CA, USA, 2015.
- [26] W. S. Noble. What is a support vector machine? *Nature biotechnology*, 24(12):1565–1567, 2006.
- [27] F. Pedregosa, G. Varoquaux, A. Gramfort, V. Michel, B. Thirion, O. Grisel, M. Blondel, P. Prettenhofer, R. Weiss, V. Dubourg, J. Vanderplas, A. Passos, D. Cournapeau, M. Brucher, M. Perrot, and E. Duchesnay. Scikit-learn: Machine learning in Python. *Journal of Machine Learning Research*, 12:2825–2830, 2011.

- [28] N. Perraudin, A. Srivastava, A. Lucchi, T. Kacprzak, T. Hofmann, and A. Réfrégier. Cosmological n-body simulations: a challenge for scalable generative models, 2019.
- [29] W. H. Press and P. Schechter. Formation of Galaxies and Clusters of Galaxies by Self-Similar Gravitational Condensation. *Astrophysical Journal*, 187:425–438, Feb. 1974.
- [30] J. R. Quinlan. Induction of decision trees. *Machine learning*, 1(1):81–106, 1986.
- [31] J. D. Rennie, L. Shih, J. Teevan, and D. R. Karger. Tackling the poor assumptions of naive bayes text classifiers. In *Proceedings of the 20th international conference on machine learning (ICML-03)*, pages 616–623, 2003.
- [32] J. d. D. Rojas Olvera, I. Gómez-Vargas, and J. A. Vázquez. Observational cosmology with artificial neural networks. *Universe*, 8(2):120. [arXiv:2112.12645], 2022.
- [33] A. J. Smola and B. Schölkopf. A tutorial on support vector regression. *Statistics and computing*, 14(3):199–222, 2004.
- [34] V. Springel. The cosmological simulation code GADGET-2. *mnras*, 364(4):1105–1134, Dec. 2005.
- [35] X. Xu, S. Ho, H. Trac, J. Schneider, B. Poczos, and M. Ntampaka. A First Look at Creating Mock Catalogs with Machine Learning Techniques. *Astrophysical Journal*, 772(2):147, Aug. 2013.